

Article

Analysis of Grid-Scale Photovoltaic Plants Incorporating Battery Storage with Daily Constant Setpoints

Juan A. Tejero-Gómez  and Ángel A. Bayod-Rújula * 

Department of Electrical Engineering, University of Zaragoza, 50018 Zaragoza, Spain; jatejero@unizar.es

* Correspondence: aabayod@unizar.es

Abstract: A global energy transition is crucial to combat climate change, involving a shift from fossil fuels to renewable sources and low-emission technologies. Solar photovoltaic technology has grown exponentially in the last decade, establishing itself as a cost-effective and sustainable option for electricity generation. However, its large-scale integration faces challenges due to its intermittency and lack of dispatchability. This study evaluates, from an energy perspective, the case of hybrid photovoltaic (PV) plants with battery storage systems. It addresses an aspect little explored in the literature: the sizing of battery storage to maintain a steady and constant 24 h power supply, which is usually avoided due to its high cost. Although the current economic feasibility is limited, the rapidly falling price of lithium batteries suggests that this solution could be viable in the near future. Using Matlab simulations, the system's ability to deliver a constant energy production of electricity is assessed. Energy indicators are used to identify the optimal system size under different scenarios and power setpoints. The results determine the optimal storage size to supply a constant power that covers all or a large part of the daily PV generation, achieving steady and reliable electricity production. In addition, the impact of using setpoints at different time horizons is assessed. This approach has the potential to redefine the perception of solar PV, making it a dispatchable energy source, improving its integration into the electricity grid, and supporting the transition to more sustainable and resilient energy systems.

Keywords: firm power generation; firm capacity; day-ahead; renewable integration; PV integration; battery energy storage system



Citation: Tejero-Gómez, J.A.; Bayod-Rújula, Á.A. Analysis of Grid-Scale Photovoltaic Plants Incorporating Battery Storage with Daily Constant Setpoints. *Energies* **2024**, *17*, 6117. <https://doi.org/10.3390/en17236117>

Academic Editors: Cecilia Boström, Irina Temiz and Janaína Gonçalves De Oliveira

Received: 13 November 2024

Revised: 1 December 2024

Accepted: 2 December 2024

Published: 5 December 2024



Copyright: © 2024 by the authors. Licensee MDPI, Basel, Switzerland. This article is an open access article distributed under the terms and conditions of the Creative Commons Attribution (CC BY) license (<https://creativecommons.org/licenses/by/4.0/>).

1. Introduction

The global energy transition is essential to address the challenges of climate change. This process involves replacing an energy system based on fossil fuels with one dominated by renewable energy sources and low-carbon technologies [1]. In this context, the International Energy Agency (IEA), in its report [2], proposes a roadmap for the global energy sector to achieve net zero carbon emissions by 2050. This plan calls for a profound and unprecedented transformation in energy production and consumption, including the phasing out of fossil fuel use and a massive expansion of renewable energy. The International Renewable Energy Agency (IRENA) in [3] estimates that an accelerated transition to renewables could reduce CO₂ emissions in the energy sector by up to 70% by 2050. This would result in a reduction of up to 37 Gigatonnes of annual CO₂ emissions by that date. The international community has recognised the urgency of addressing the problem of climate change and has established a series of commitments and agreements to mitigate its effects and adapt to its inevitable consequences. Key international commitments include the Paris Agreement [4] and the United Nations 2030 Agenda [5].

Solar photovoltaic technology has rapidly become one of the most economical ways to generate electricity. In recent years, its worldwide expansion has been exponential. This technology is an essential pillar in the transition to more sustainable energy systems. According to the International Renewable Energy Agency (IRENA), the installed capacity

of photovoltaic energy has grown from 175 GW in 2013 to more than 1410 GW in 2023 [6], representing an increase of more than 800% in a decade. This growth is attributed to several factors. First, cost reductions. According to data from the International Renewable Energy Agency (IRENA), the average global levelised cost of electricity (LCOE) for large-scale solar power projects was \$0.044/kWh in 2023, representing a 90% drop since 2010 [7]. Second, international commitments such as the Paris Agreement [4] and the Sustainable Development Goals [5]. Thirdly, favourable government policies, as many countries have introduced incentives that promote their installation. Finally, solar PV is highly scalable, meaning that it can be applied in a wide variety of projects, from small residential installations to large industrial plants.

Reducing the intermittency of renewable resources has been a topic of great interest and continues to generate a significant amount of literature. Solar energy is inherently nondispatchable due to the variability associated with natural factors such as the Earth's rotation and cloud movement. Before PV production had a significant impact on the electricity system, its variability was considered tolerable. However, as cumulative installed PV power has increased, it has become necessary to implement measures to mitigate this intermittency. This involves optimising the scheduling of the expected PV production in the power system or applying limitations on its generation [8].

Power plants face economic penalties when there are deviations between the amount of energy they commit to deliver and the actual amount delivered. Using deep learning techniques, as described in the study [9], it is possible to determine the minimum battery capacity necessary for PV plants to consolidate their energy production throughout the day. In addition, variations in irradiance caused by changes in cloud cover can lead to rapid power fluctuations in PV plants. Energy storage systems are often used to mitigate these power fluctuations in the grid using various control algorithms [10].

To improve the integration of large-scale renewable generation systems, there are several prominent options, such as pumped hydro storage, solutions that convert surplus generation into thermal energy, and hydrogen or mobility applications, which are receiving considerable attention [11]. Among the solutions most compatible with solar generation are lithium-ion batteries [12]. They are a promising option for use in grid-level energy storage systems. This is due to their flexibility for installation, high efficiency (85–95%), high energy density (75–250 Wh/kg), low self-discharge rate (0.1–0.3%) and their fast response capability [13,14]. In [15], levelised costs for grid-scale PV combined with lithium-ion batteries are estimated at 0.17 to 0.36 EUR/kWh.

Another promising storage technology is vanadium redox batteries. These batteries stand out for their high scalability, efficiency and long lifetime, which makes them an attractive option for renewable energy applications [16]. The main challenge is their high initial cost, influenced by the price of vanadium and their low energy density.

In [9], the minimum size of the battery energy storage system (BESS) required to guarantee the firm capacity of PV plants in the intraday market is investigated. Firm capacity technologies are energy sources whose capacity is available during most generation periods. These sources are controllable and can supply power as needed regardless of weather or other external conditions [17]. This is essential to safeguard the stability of the power system. In [17], the firm capacity coefficient is quantified for various generation technologies. Nuclear power, with a coefficient of 0.97, and open cycle gas turbine (0.96) have a high reliability of power supply. In contrast, solar PV has a value of 0, suggesting that it cannot be considered a reliable source. Pumped hydro storage has a value of 0.77, reflecting its efficiency in providing firm energy. In this study, the aim is to achieve a quasi-firm capacity of 1, i.e., to ensure that the system under analysis can constantly and reliably provide all the energy required (similar to nuclear power). Firm power generation is essential to enable a high penetration of photovoltaics and, thus, the gradual replacement of conventional power generation. A PV system that can guarantee predictable, constant power production is classified as firm generation. In the following, some studies that aim to provide firmness in power supply with PV generation are presented.

In [18], a “firm kWh” is defined as a kWh of energy that can meet demand specifications with 100% certainty. To mitigate intermittency and provide stable PV generation at the lowest cost, it is crucial to oversize the PV installation and reduce production. In addition, the geographical dispersion of PV installations helps to reduce generation variability. To mitigate the intermittency of solar PV, a BESS of 873 kWh for a 1.3 MWp PV plant is implemented in [19]. In [20], the storage required to mitigate the mismatch between energy demand and solar PV generation is analysed. It concludes that to balance the mismatch in intervals of a few hours, between 2 and 7 GWh of storage capacity is required for each GW of installed PV capacity. Battery storage continues to present a significant economic challenge compared to wind, PV, gas or coal energy sources when evaluated in terms of levelised cost of electricity (LCOE) [21]. As battery technology continues to evolve and production costs decrease, it is possible that in the medium term, batteries will become more competitive. In [21], a reduction of the LCOE by approximately 83% over the last 10 years from around \$900/MWh to \$150/MWh is observed.

Energy arbitrage or PV production forecasting to optimise the use of storage is widely explored in the literature, especially now that these solutions are becoming economically viable. However, to date, the goal of providing a constant energy supply with PV plants with storage has not been feasible, mainly for economic reasons. The continuous decrease in costs of battery storage systems opens up the possibility that, in the medium term, such a strategy can be envisaged. This is particularly relevant in scenarios where the integration of more PV generation into the grid is limited by technical or capacity constraints. This paper aims to provide a new perspective not addressed in the literature on PV-BESS hybrid plants, moving away from approaches focused solely on economic analyses. It is part of an ongoing line of research that aims to determine the degree of robustness that a large-scale photovoltaic system with energy storage can offer to the grid.

Robustness, in this context, is defined as the ability of the system to guarantee a constant and reliable power supply. This characteristic is crucial for the effective integration of renewable generation into the electricity system, especially considering that sources such as solar are intermittent due to weather variables and diurnal cycles. In previous studies of the authors, the performance of a hybrid photovoltaic plant with energy storage was evaluated, analysing its ability to meet operational setpoints over different time horizons. Scenarios with annual setpoints were considered in [22], where a constant power level was sought throughout the year, and monthly setpoints in [23,24], which allow for finer adjustments of the power setpoint according to seasonal variations in power generation.

The intraday market that exists in many countries (as is the case of Spain) allows electricity supply and demand to be adjusted in near real time after the close of the daily market. It facilitates the correction of unforeseen deviations in generation or consumption, ensuring the stability of the system, and is especially useful for integrating renewable energies with variable production. Intraday auctions, like the day-ahead market, follow the marginalist model and the market coupling model for the borders it manages. The intraday auction market in Spain is organised in three sessions. This paper proposes to participate in the second auction, which closes the session at 22:00 h and performs price matching at 22:20 h. This auction schedules energy for 24 h the following day [25].

The aim of this study is to analyse, from an energy point of view, the behaviour of a hybrid PV plant with battery storage. The remainder of this paper is structured as follows: Section 2 describes the proposed model together with its parameters and indicators; Section 3 presents the results of the analysis carried out; finally, the conclusions are presented in Section 4.

2. Methodology

2.1. Formulation and Hypothesis of the Proposed Problem

The aim of this study is to analyse, from an energy point of view, the behaviour of a hybrid PV plant with battery storage. Solar PV energy has an intrinsically variable production that is dependent on the daily cycle of the sun. The typical PV generation

profile is bell-shaped, concentrating its maximum output in the central hours of the day and gradually decreasing towards sunrise and sunset. This variability poses significant challenges for grid integration, especially when seeking to ensure a continuous and reliable supply of energy.

This study proposes to transform the classical production profile (PV in Figure 1) into a profile with a constant energy supply 24 h a day (SUPPLY in Figure 1). This supply mode is sometimes referred to in the literature as “baseload” [15]. By storing the surplus energy generated during the hours of highest solar radiation, it is possible to release the stored energy during the rest of the day, maintaining a constant power output of the system.

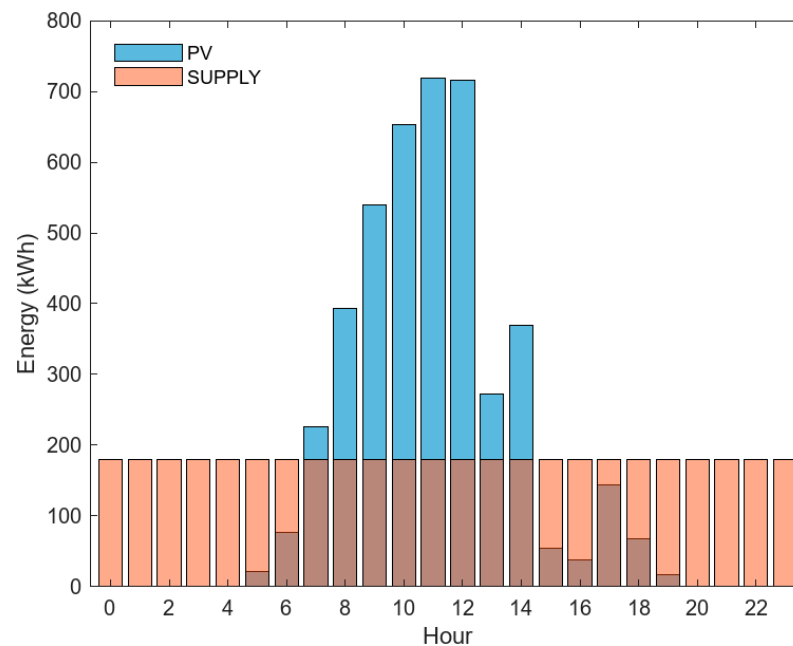


Figure 1. Hourly power generated (PV) and system power supply (SUPPLY) for one day.

The energy analysis of this system involves evaluating various parameters, resulting in energy indicators that determine the optimal installation size. The central hypothesis is that, by properly sizing the storage system, it is possible to provide a constant power setpoint with high availability guarantees. This would imply that the hybrid PV plant can overcome the limitations of intermittency and variability inherent to solar generation.

2.2. Software Tool and Source Data

The algorithm was developed and the calculations necessary to perform this analysis were carried out using MATLAB R2023a [26]. The production of the photovoltaic installation is evaluated using hourly data of solar irradiance incident on the plane of the photovoltaic module and the ambient temperature. These data are obtained from the PVGIS-SARAH2 database [27]. In this case, the School of Engineering and Architecture of the University of Zaragoza, Calle María de Luna, Zaragoza, has been selected as the geographical reference point. To ensure an accurate assessment, an analysis of hourly data over a solar period spanning approximately 11 years is carried out. Specifically, data from 1 January 2010 to 31 December 2020 is examined. The long-term analysis of PV production shows a tendency to neutralise annual fluctuations. A fixed mounting for the PV modules with an adjusted slope and azimuth is selected to optimise the yield at the proposed location. 550 W FS-7550A-TR1 PV modules manufactured by First Solar (Tempe, AZ, USA) have been chosen [28]. The PV plant is composed of 1818 modules, providing a total peak power of 999.9 kWp.

2.3. Development and Description of the Proposed Model

Consistent with previous research [22–24], the present study continues with the analysis of the behaviour of a PV plant with storage. The analysed model was proposed in [24]. The BESS can inject energy when the PV plant does not meet the setpoint or store the surplus. Figure 2 shows the summarised flowchart of the proposed model, in which the stages involved in the operation of the algorithm are detailed.

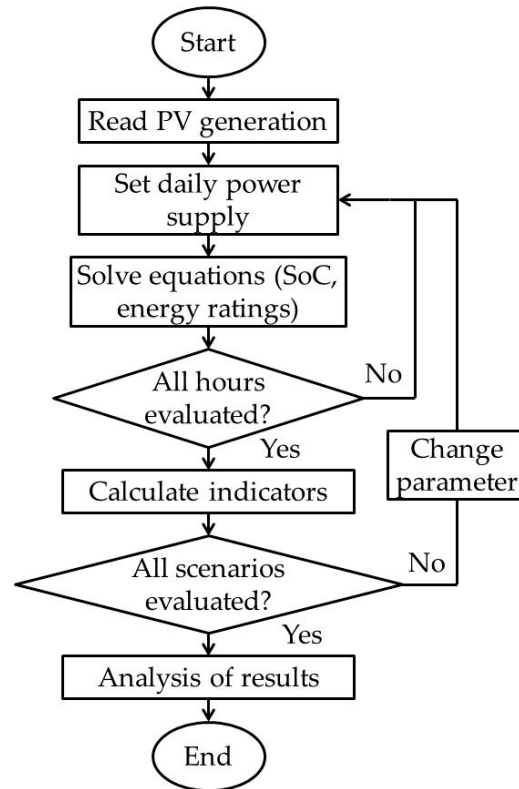


Figure 2. Flowchart of the model.

For the sake of brevity and considering that this study is a continuation of [24], the main equations used by the algorithm that are evaluated in hourly intervals are summarised in (1).

$$\begin{aligned}
 T_C &= T_A + G_M \cdot \frac{NOCT - 20}{800} \\
 P_{MOD} &= P_N \cdot G_M \cdot \frac{(1 + \gamma \cdot (T_C - 25))}{G_{STC}} \\
 E_{PV} &= N_P \cdot P_{MOD} \cdot C_{LOSS} \cdot T_S \\
 E_{B,t} &= \begin{cases} E_{B,t-1} \cdot (1 - \sigma) - \Delta t \cdot \eta_{B,EF} \cdot (P_{PV,t} - \frac{P_{BC,t}}{\eta_{B,INV}}) & t \in \text{charging} \\ E_{B,t-1} \cdot (1 - \sigma) - (\Delta t \cdot \frac{P_{BD,t}}{\eta_{B,INV}} - P_{PV,t}) & t \in \text{discharging} \end{cases}
 \end{aligned} \quad (1)$$

Session 3 of the Spanish intraday market starts at 21:00 h (legal time). At this time, precise data on the energy produced during that day are already available because sunset has been reached. Similarly, the amount of constant power supplied during this day is also known because it was set at 0:00 h, which allows us to determine the exact energy stored in the BESS at the end of the day. At 22:20 h, the next day's 24 h schedule is published. With a reliable forecast of the expected solar radiation for the next day, during session 3 of the intraday market, it is possible to estimate a reliable constant power setpoint for the next day. A snapshot illustrating the described case is presented in Figure 3.

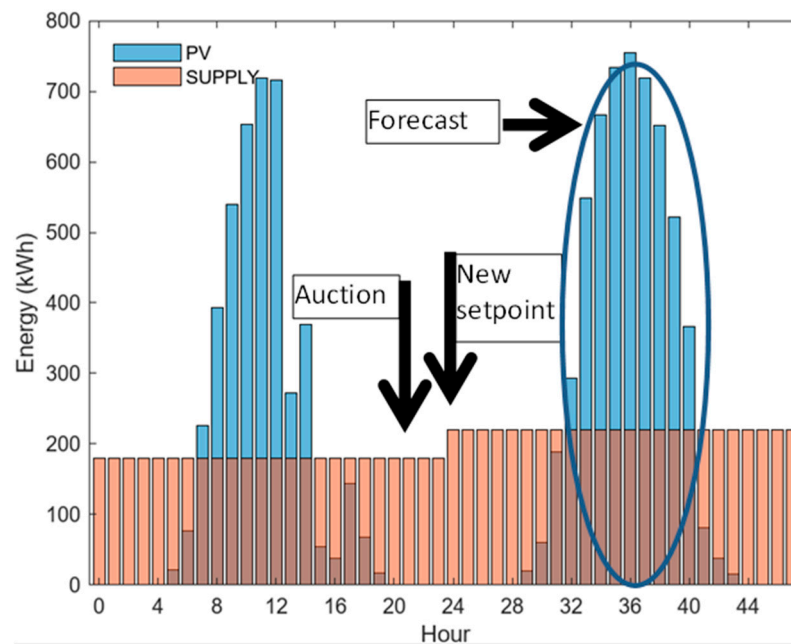


Figure 3. Hourly power generated (PV) and system power supply (SUPPLY) for two days.

In a step prior to the main simulation, the PV production is determined for the whole period. Each hour, the PV power generation is calculated using E_{PV} from Equation (1). Assuming that the weather forecast is accurate, every day at 22:00 h, during session 3 of the intraday market, the constant power setpoint for the following day is defined. This setpoint is constant for the 24 h of the following day, and the sum of energy to be supplied is equivalent to the average PV generation expected for the following day. In this way, each day, an amount of energy equivalent to the PV production expected on the same day is supplied. This is an ambitious target as the aim is to supply the entire PV production generated as constant power for 24 h. The State of Charge (SoC) in the BESS is calculated according to Equation (1), where $(E_{B,t})$ represents the energy stored in the BESS. The BESS is subject to a maximum capacity constraint, which depends on its nominal value, and a minimum capacity, which is 10% of the nominal capacity.

Finally, since the simulation is carried out over a long period of time, it is essential to include the degradation phenomena of the storage system in the model. Degradation in batteries is due to two components: cycling ageing and calendar ageing. For both components, the degradation models of [24] have been used. Calendar ageing only takes into account the time variable, while cycling ageing depends on the type of storage charging and discharging. In the algorithm, a function is incorporated that calculates the equivalent cycles of charge and discharge of the BESS using the rainflow-counting method. This method is implemented in a similar way as described in [24]. Each half-cycle provides information on the depth of discharge and its mean value, from which the cycling degradation is calculated. As a result, multiple energy indicator matrices are generated, which depend on various parameters, such as the storage size and the amount of energy to be supplied. These results are discussed in Section 3.

The repeatability of all analyses performed in this study is guaranteed, as the developed algorithm always uses the PVGIS radiation database at the same geographical point as the source data.

2.4. Study Parameters and Indicators

The following parameters and indicators are used for this analysis, some of which have been previously used in [23,24]. The reason for their continued use is to provide consistency in the ongoing research and to allow comparisons with previous studies.

The parameter $S2P$ represents the relative storage capacity of the system. It is defined in Equation (2), where C_{MAX} is the capacity of the BESS and P_p is the peak power of the PV plant. The $S2P$ parameter, being relative, allows the size of the PV plant to be decoupled from the energy storage capacity. To illustrate the storage capacity in a specific application with an $S2P$ of 1, two examples are provided. First, in a residential PV plant with a photovoltaic coverage of 405 m² and an installed capacity of 40.3 kWp [29], the required energy storage in batteries would be 40.3 kWh. Second, in a grid-scale PV plant composed of 10 parallel groups of arrays with a power rating of 2 MWp [30], an equivalent storage of 2 MWh would be needed. These examples reflect how the $S2P$ parameter relates to storage capacity.

$$S2P = \frac{C_{MAX}}{P_p} \quad (2)$$

In Equation (3), the parameter K_{SUPPLY} is defined where E_{SUPPLY} is the hourly energy setpoint supplied by the system, and E_{PV} is the PV energy produced for that hour. The K_{SUPPLY} parameter represents a quantitative relationship between the power to be supplied and the expected PV generation for a given day. It is a coefficient that indicates how the delivered power matches the available PV generation potential. This parameter varies between 0 and 1, where $K_{SUPPLY} = 1$ indicates that the total generated PV output of a day is equivalent to the power to be supplied on that day.

$$K_{SUPPLY} = \frac{\sum_{h=0}^{h=23} E_{SUPPLY,h}}{\sum_{h=0}^{h=23} E_{PV,h}} \quad (3)$$

The State of Charge (SoC) is an indicator that reflects the charge level of an energy storage system in relation to its total capacity. This indicator is expressed in percentage terms, representing the amount of energy remaining in the battery at a specific point in time. In this paper, the SoC operating range is considered to be between 10% and 100%, values commonly applied in storage systems using lithium batteries [31].

State of Health (SoH) is an indicator that reflects the maximum usable capacity of the current cycle of the battery compared to its initial rated capacity [32]. This qualitative measure indicates the degree of degradation that translates into decreases in capacity and performance.

The indicators used below represent annual average values for the entire simulation period. They are, therefore, consistent data, as they are generally averaged over a period of up to 11 years.

In Equation (4), the AED (Annual Energy Deviation) indicator is defined as the quotient between the unavailable energy and the energy to be supplied during the entire simulation period. E_{PV} represents the PV generation in each hour, E_{GRID} represents the energy supplied, and h represents the number of hourly periods of the simulation.

$$AED = \frac{\left| \sum_{h=1}^{h=96,360} (E_{PV} - E_{GRID}) \right|}{\sum_{h=1}^{h=96,360} E_{GRID}} \vee \left(\sum_{h=1}^{h=96,360} (E_{PV} - E_{GRID}) < 0 \right) \quad (4)$$

The MED (Monthly Energy Deviation) indicator is defined in a similar way to the AED indicator, but it disaggregates the data by month. Therefore, the same calculation is performed for each month as in Equation (4).

The AEE indicator, described in Equation (5), is analogous to the AED indicator, with the difference that, instead of calculating energy deficits, it computes excess energy in the system.

$$AEE = \frac{\left| \sum_{h=1}^{h=96,360} (E_{GRID} - E_{PV}) \right|}{\sum_{h=1}^{h=96,360} E_{GRID}} \vee \left(\sum_{h=1}^{h=96,360} (E_{PV} - E_{GRID}) > 0 \right) \quad (5)$$

2.5. Limitations of the Method

The proposed analysis uses historical radiation data from the PVGIS database in order to compare the current results with the current line of research. It is important to note that possible interruptions in the operation of the PV plant, either due to maintenance or system failures, are not considered. Consequently, the PV production data presented should be understood as an approximation that reflects the most favourable possible scenario, as it does not take into account any type of operational inconvenience.

The PV production forecast for the following day is assumed to be highly accurate. Nowadays, advanced techniques, such as those based on artificial neural networks [33–35], allow accurate estimation of solar radiation and, thus, PV energy production at a given point. Also, meteorological models such as the European Centre for Medium-Range Weather Forecasts [36] or the Weather Research and Forecasting Model [37] provide accurate estimates of future weather conditions. Therefore, the PV energy production expected in the forecast is considered to closely match what will actually be generated under real conditions.

3. Results

This section presents the most relevant results of the simulation proposed in Section 2. The AED and MED indicators are used to evaluate the system behaviour and determine the appropriate storage size for each power setpoint and scenario. In addition, the results of this study are compared with previous research, which allows significant improvements to be identified when applying the daily power setpoint.

The algorithm designed in MATLAB performs hourly energy assessments, calculating the energy unavailability at each hour. This unavailability occurs when the system cannot supply the scheduled power (setpoint power). Specifically, it occurs when the sum of the PV production for that hour and the energy available in the storage system is less than the energy setpoint that must be supplied during that hour. Although the daily power setpoint is calculated in an attempt to match the estimated PV production, not all PV production can be stored if the BESS is not sufficiently sized. Therefore, the surplus energy that cannot be stored becomes unavailable energy that cannot be supplied in later hours.

3.1. MED Indicator Analysis

The MED indicator, as defined in Section 2, provides a detailed disaggregation of monthly energy unavailability. This allows for a more accurate analysis of the variability in energy supply throughout the year, facilitating the identification of patterns in energy unavailability.

Since the PV production forecast will be accurate on a daily basis, it is expected that the energy supplied by the system will not deviate, as the power setpoint is adjusted on a daily basis. This situation is consistent throughout the year, so the MED indicator should maintain some monthly uniformity, as the power supply continuously adapts to the PV production.

When analysing the data presented in Figure 4, a significant variability in the MED indicator is observed. In particular, during the summer months (June, July and August) and in the winter months (December and January), the MED indicator is significantly lower. The three-dimensional surface plots in Figure 4 show the MED indicator as a function of the month of the year and the K_{SUPPLY} parameter. The simulation of each case is carried out until the storage system reaches the end of life. Figure 4a shows a curve for a very low storage size ($S2P = 1$). Figure 4b shows a medium storage ($S2P = 3$), and Figure 4c shows a high storage ($S2P = 5$). Although $S2P = 5$ may seem high, it is within the estimates of other similar studies. For instance, the study [38] estimates that for an 8.6 MW PV plant, a 44 MWh battery is needed, which is equivalent to an $S2P$ ratio of 5.1 to cover the demand.

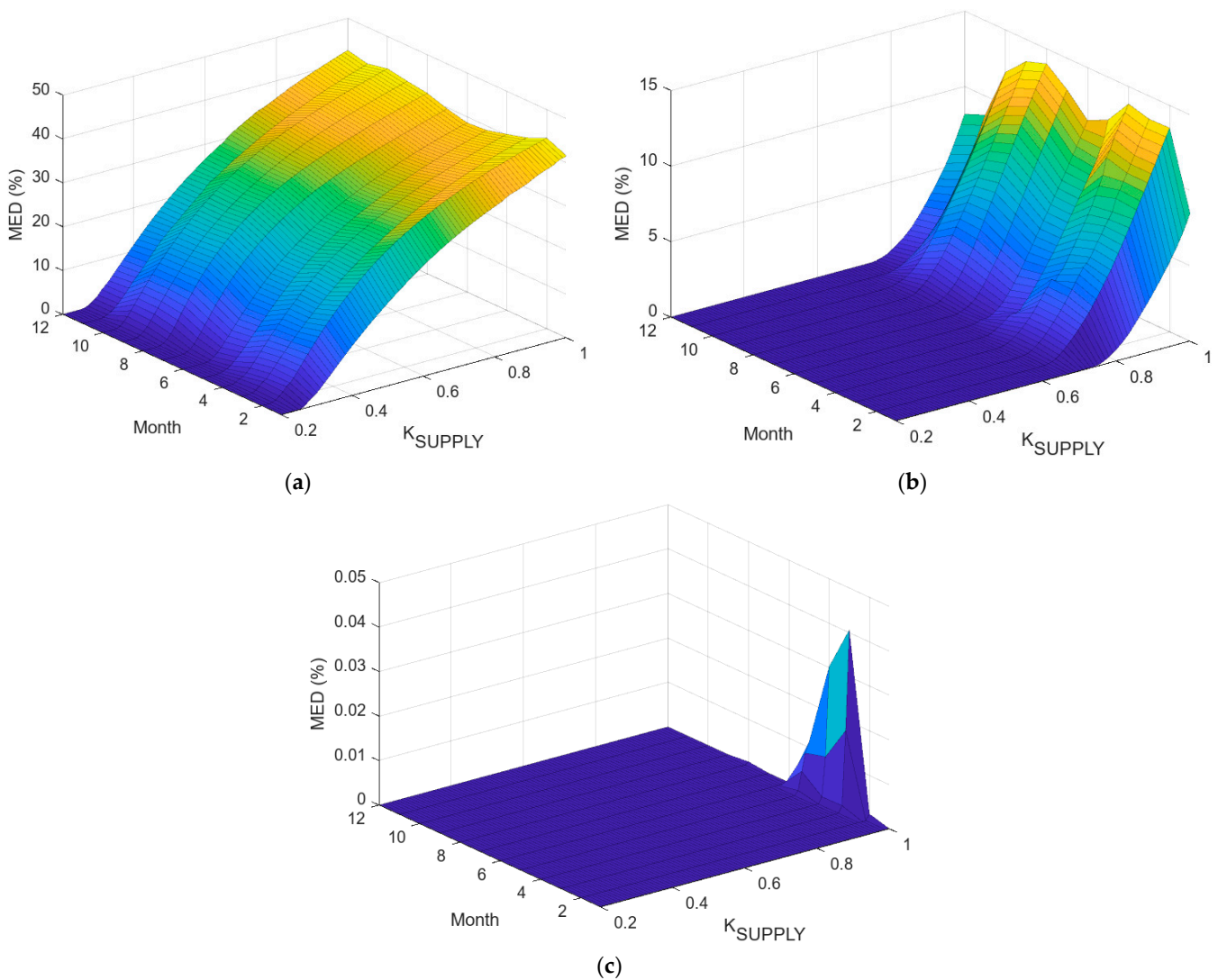


Figure 4. MED indicator as a function of power setpoint with simulation. (a) $S2P = 1$; (b) $S2P = 3$; (c) $S2P = 5$.

It is understandable that the MED indicator is lower in the months of December and January, as the PV production is lower in that period, which reduces the power setpoint to be delivered. As a result, the power setpoint to be provided by the BESS each day tends to equalise with the amount of energy that can be stored in the BESS.

To verify this assumption, Figure 5 presents three graphs with energy results for each significant period of the year (winter, summer and the transition between the two seasons).

The red bars (PV) represent the daily PV energy production, while the blue bars (DEF) indicate the energy unavailability of the system. For the sake of clarity, the setpoint daily power values are not included in Figure 5, but their value can be calculated as the difference between the photovoltaic production (PV) and the energy deficit (DEV) represented in the figure. Figure 5a, corresponding to the month of January, shows that significant energy unavailability occurs only on those days with high PV production (days 9, 20, 22, 26, 27, 28). On the other hand, all the days in which PV production is less than 4 MWh present zero energy unavailability.

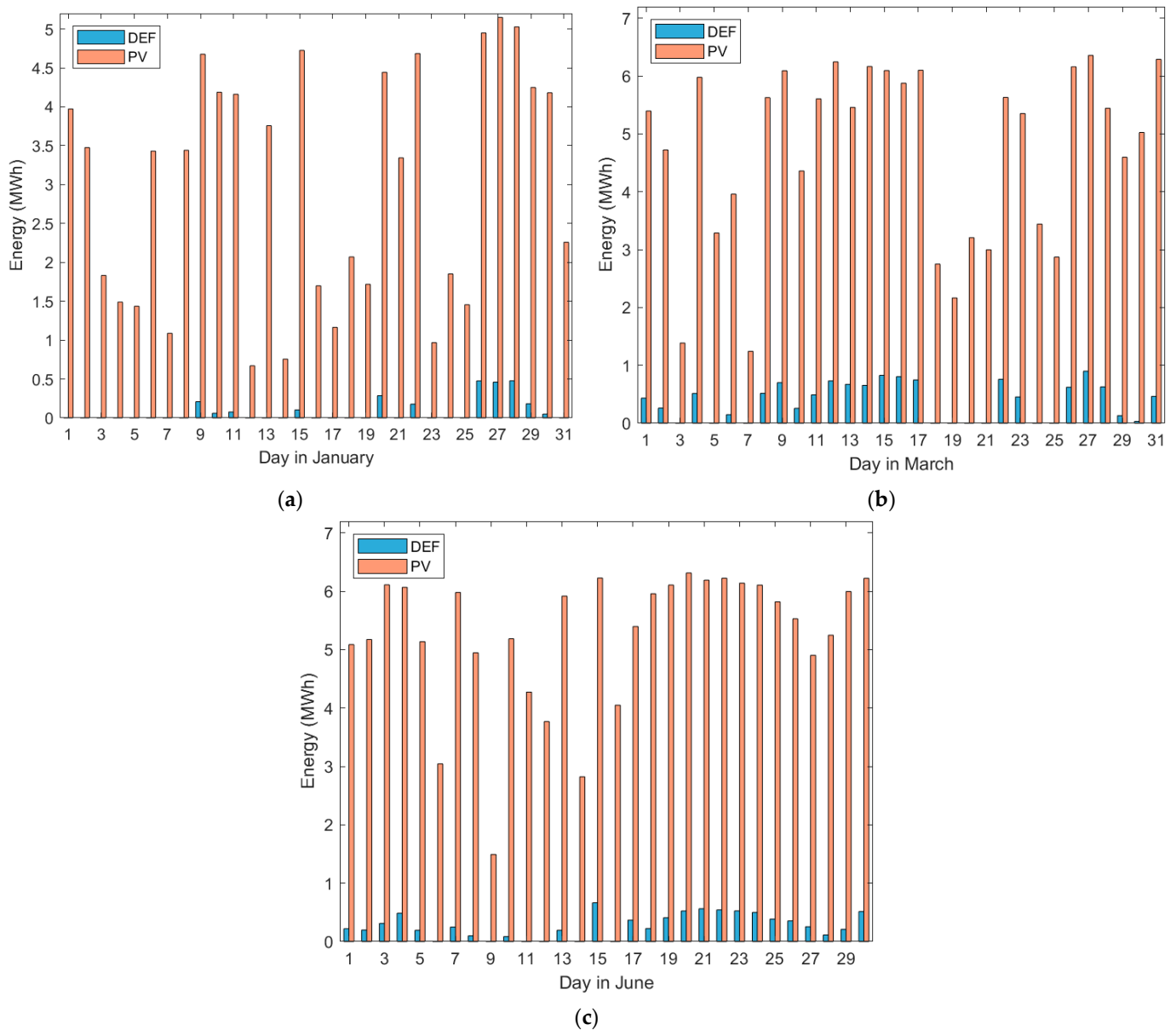


Figure 5. PV generation and daily energy unavailability. (a) Month of January; (b) month of March; (c) month of June.

Figure 5b shows the month of March. Since PV production is higher in March, the power setpoint also increases, resulting in higher energy unavailability. Only days 7, 18, 19, 20, 21, 24 and 25 do not present energy unavailability, as PV production on these days is lower. This situation explains why the MED indicator is higher in March and April compared to December and January.

It would be expected that in June the MED indicator would follow an upward trend and be higher than in March, given that PV production is significantly higher. However, as shown in Figure 5c, the unavailability in June is lower than in March.

To understand why the MED indicator does not reach peak values in June or July, the behaviour of the BESS is analysed for 4 typical days in March and another 4 days in June, as shown in Figure 6 for an intermediate storage size ($S2P = 3$). An intermediate value of the $S2P$ coefficient is selected because it allows us to observe the contrast between days when the energy supply can be met and those when it cannot. If the $S2P$ were too low or too high, there would be unavailability practically every day or never, respectively. Extreme storage sizes are not representative and blur the effect we aim to analyse.

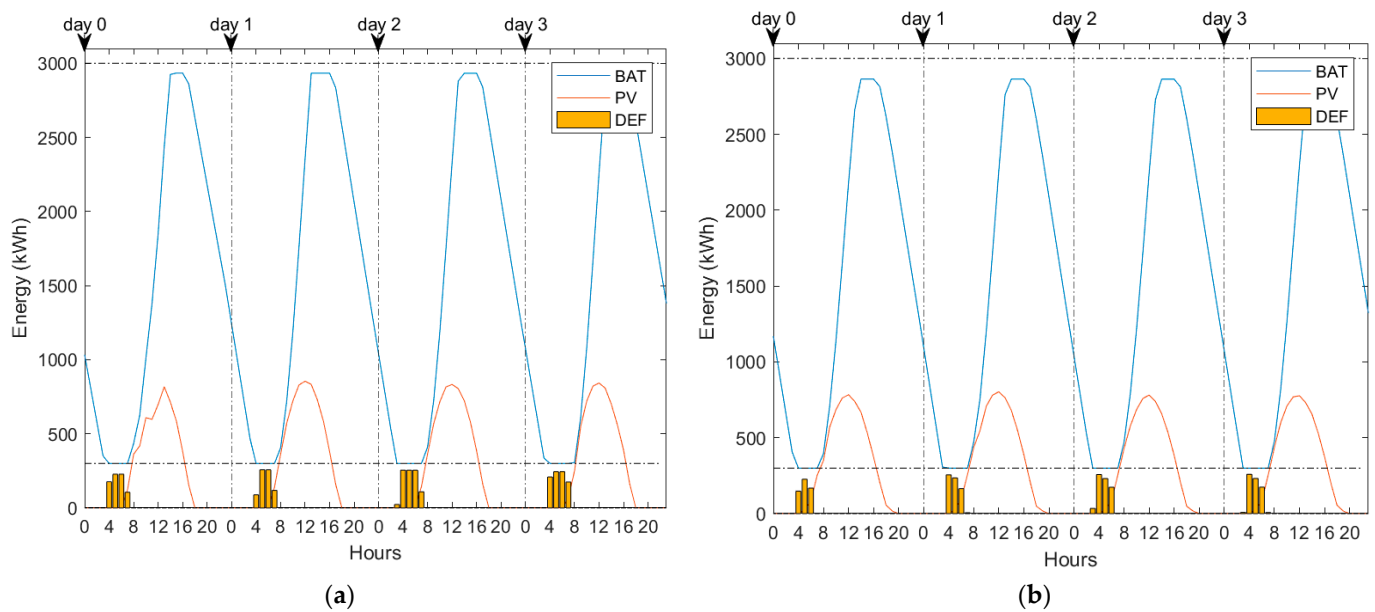


Figure 6. Energy stored in BESS, PV generation and hourly energy unavailability for S2P of 3. (a) March; (b) June. DEF = energy deficit.

In Figure 6, the blue curve represents the energy available in the BESS, the orange curve represents the PV production and the yellow bars reflect the energy unavailability of the system. Figure 6a, corresponding to March, shows that there are energy unavailabilities every day during the early morning hours, lasting for three to four hours. This is because the BESS does not have sufficient capacity to maintain a high constant power supply for so many hours, from sunset to sunrise.

In June, although PV production is at its highest and constant power is supplied even higher than in March, there are more hours of PV production during the day. Early in the morning, energy unavailability can be neutralised because renewable resources are already available. This allows for a more stable and continuous power supply and is the reason why MED in June or July goes down rather than up, despite having a higher power setpoint than in March.

In Figure 6, simulations are shown to illustrate the behaviour of energy unavailability on two specific days. Every hour in which the PV plant with battery storage cannot meet the scheduled power setpoint due to the absence of PV production and the lack of energy stored in the BESS is counted as an hour of energy unavailability. Since the simulation spans several years until the end of the BESS's life, Figure 7 shows an annual average of this unavailability hour counter. The results are classified by hour of the day (0:00 h to 23:00 h) and month of the year (January to December) and represent the number of days with energy unavailability broken down by hours. These results allow for a more reliable observation of the effects of seasonality and the timing of occurrences. The results in Figure 7 match in magnitude with those in Figure 6 and support the conclusions drawn.

Firstly, the effect of seasonality is observed: in April, at 6:00 h., more hours of energy unavailability are recorded (29.79 days) compared to January (17.58 days) due to a lower power target in the latter. Likewise, a reduction in hours of unavailability is observed between 7:00 h and 9:00 h during the summer, as there is greater availability of photovoltaic resources early in the morning compared to winter.

Secondly, the hourly distribution of energy unavailability is observed: in July, the hours of unavailability are concentrated within a narrower time interval compared to the autumn or spring seasons.

In conclusion, it is significant to note that, although in June, there is a high PV production and the power setpoint is more demanding for the BESS, the higher availability of renewable resource hours contributes to reducing the MED indicator.

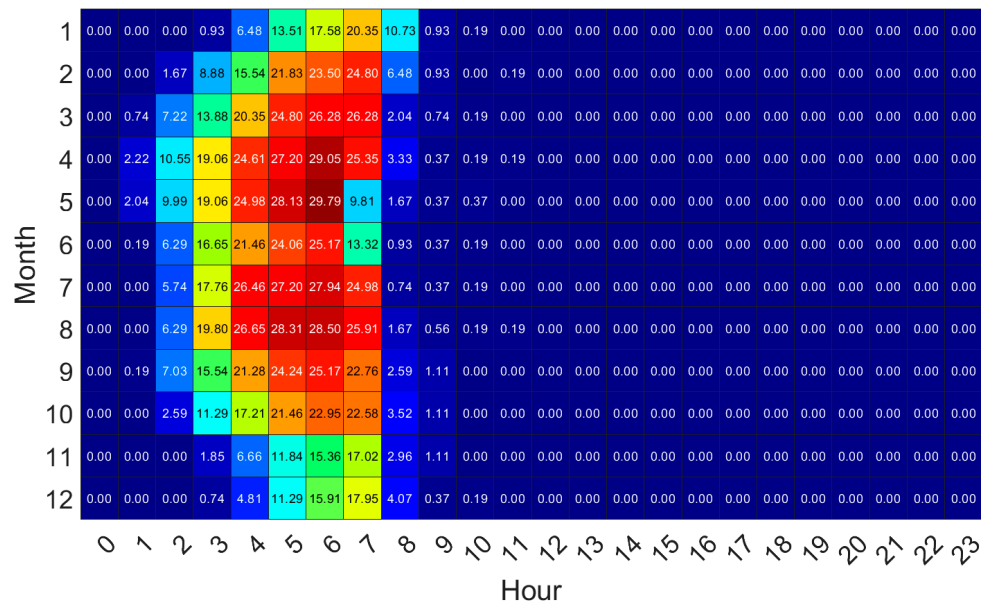


Figure 7. Average days of unavailability by month and hour of the day up to end of life.

Every hour in which PV production exceeds the sum of the energy that can be stored in the BESS and the energy supplied to the grid as constant power is counted as an hour of energy surplus. Since the simulation spans several years until the end of the BESS’s lifespan, Figure 8 shows an annual average of this surplus hour counter. The results are classified by hour of the day and month of the year, similar to Figure 7, and represent the number of days with energy surpluses broken down by hours. Energy surpluses are concentrated in the middle of the day, specifically between 13:00 h and 16:00 h, a time slot when energy holds a low economic value but with an upward price trend. Therefore, it would be feasible to sell this surplus energy. The periods of greatest surplus accumulation occur around 14:00 h, with July and August standing out, as they register energy surpluses on 12.77 out of the 31 days of the month. It is reasonable for energy surpluses to be generated in the afternoon, as the BESS has had the entire PV production period of the day to fully charge.

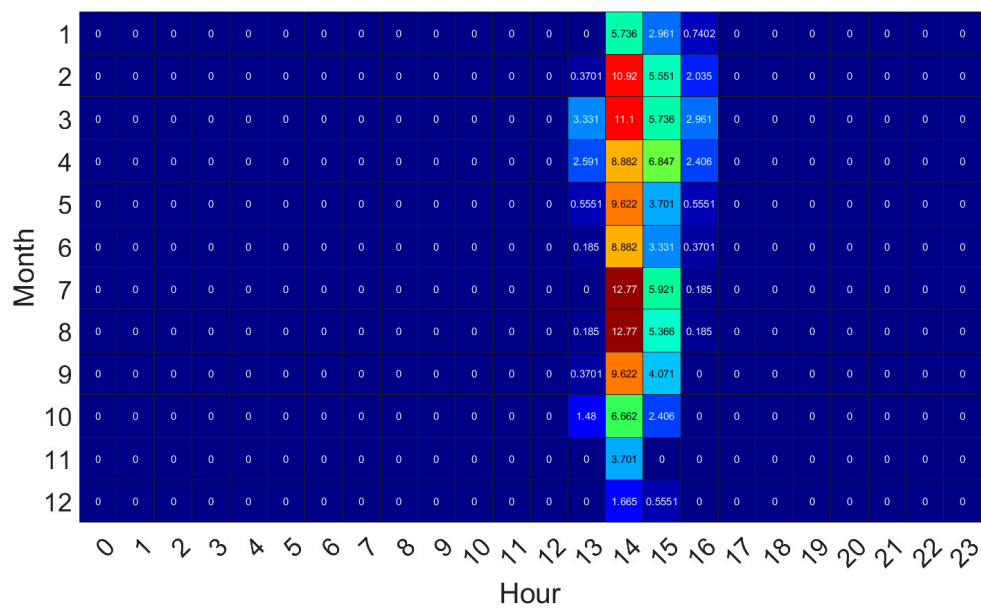


Figure 8. Average days of energy surpluses by month and hour of the day up to end of life.

3.2. Analysis of the AED Indicator

Figure 9 shows the annual unavailability deficit indicator AED. On the x -axis is the coefficient (K_{SUPPLY}), which adjusts the firm power setpoint to be supplied by the system. This graph makes it possible to quantify the influence of the storage size on the AED indicator.

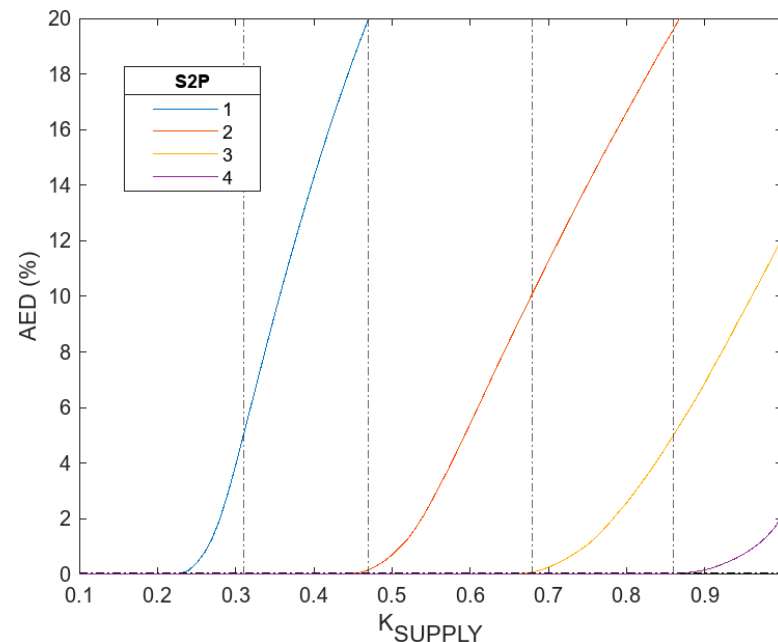


Figure 9. AED indicator as a function of power setpoint for various storage sizes.

With a very small storage size ($S2P = 1$), acceptable power availability cannot be guaranteed. For example, the AED indicator reaches 20% for a low power setpoint (K_{SUPPLY} of 0.47), which significantly limits energy supply. To decrease AED to 5%, a value close to the unavailability of a plant such as a nuclear plant providing firm power, the system could only supply a K_{SUPPLY} of 0.31, which would result in an injection over the desired setpoint of 69% of the energy generated by the PV plant.

By selecting a considerably larger storage size ($S2P = 3$), it is observed that it is possible to supply power with a K_{SUPPLY} setpoint of 0.86, keeping the AED indicator below 5%.

Furthermore, it is interesting to note that for this size of storage, power unavailability could be completely eliminated ($AED = 0$) for a K_{SUPPLY} of 0.68. This operating point, although it implies a surplus of 32% of the energy produced, offers the key advantage of transforming this PV generation into firm and reliable production.

From a storage size that can be considered oversized ($S2P = 4.6$), the system is capable of supplying all the energy generated by the PV plant at constant power, guaranteeing practically zero levels of unavailability. This indicates that this oversized storage not only optimises the utilisation of PV production but also ensures almost total energy availability, turning PV generation into a firm system.

3.3. End of Life of the Simulations

The end of life of lithium-ion batteries is reached when the capacity drops below 80% of the nominal capacity. This limit has been widely adopted by both the industry and the scientific communities because once the battery reaches this capacity level, its degradation becomes faster, and its performance is no longer suitable for most applications. Therefore, in this work, it is essential to perform the analysis until the end of life is reached rather than extending the study to the entire 11-year simulation period (96,432 h).

Figure 10 shows the number of operating hours of the BESS until it reaches the end of its lifetime. This number of hours is presented as a function of the size of the BESS and

the power setpoint to be supplied. High $S2P$ values and low power setpoints result in low depths of discharge and low degradation in the BESS. For example, for an $S2P$ of 5 and a power setpoint $K_{SUPPLY} = 0.3$, the BESS reaches the end of its lifetime at 68,000 operating hours. This behaviour is due to the fact that, with a high $S2P$ and a low power setpoint, the BESS experiences fewer deep charge/discharge cycles, reducing battery wear, which prolongs its lifetime. However, for a BESS with a relatively low capacity ($S2P = 2$) and a high power setpoint $K_{SUPPLY} = 0.8$, the end of life is reached at 45,000 h of operation. The BESS undergoes deeper and more frequent charge and discharge cycles, which increases its degradation and reduces its lifetime.

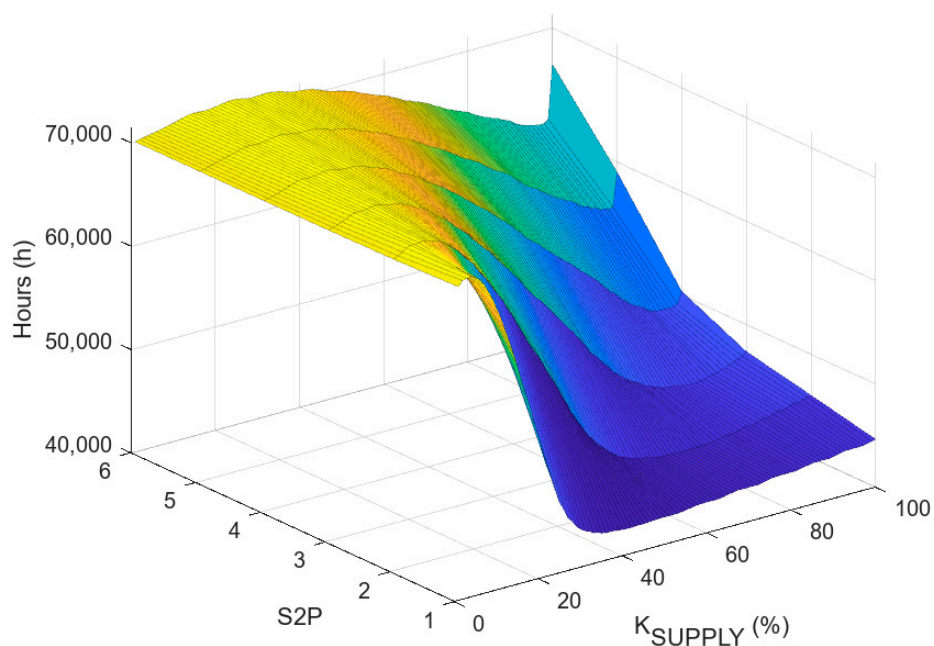


Figure 10. Number of hours to reach the end of life of the BESS.

If a high constant power value ($K_{SUPPLY} = 0.8$) is intended to be supplied, it can be seen from Figure 10 that oversizing the BESS is beneficial for the lifetime. Increasing $S2P$ from 2 to 5 leads to a significant reduction in battery degradation from 45,000 to 65,000 operating hours. This increase in storage capacity reduces the depth of discharge in each operating cycle and, therefore, the degradation of the batteries. In conclusion, for each constant power value, a maximum slope zone is observed in Figure 10, where an increase in the $S2P$ value significantly reduces the degradation of the batteries.

3.4. Comparison Between Constant Annual, Monthly and Daily Generation

The AED indicator obtained in the current study, under a daily power setpoint, can be compared with other studies, such as [24]. However, there are similar works, such as [22,23], where the model shows significant differences. In these cases, the model was not fully optimised, as they did not adequately incorporate degradation phenomena. Therefore, the results of these studies are not directly comparable with those obtained in the present study.

In order to make a rigorous comparison between the current study, which uses a daily power setpoint, and previous studies with monthly and annual setpoints, a simulation has been carried out under the same conditions. The only variable modified was the power setpoint, which was adjusted to the daily, monthly or annual cases. The purpose is to evaluate how a daily setpoint improves the monthly and annual setpoint. Figure 11 presents the results for the three scenarios, allowing a direct comparison. As expected, the daily setpoint improves the AED indicator, regardless of the storage size and the power setpoint used.

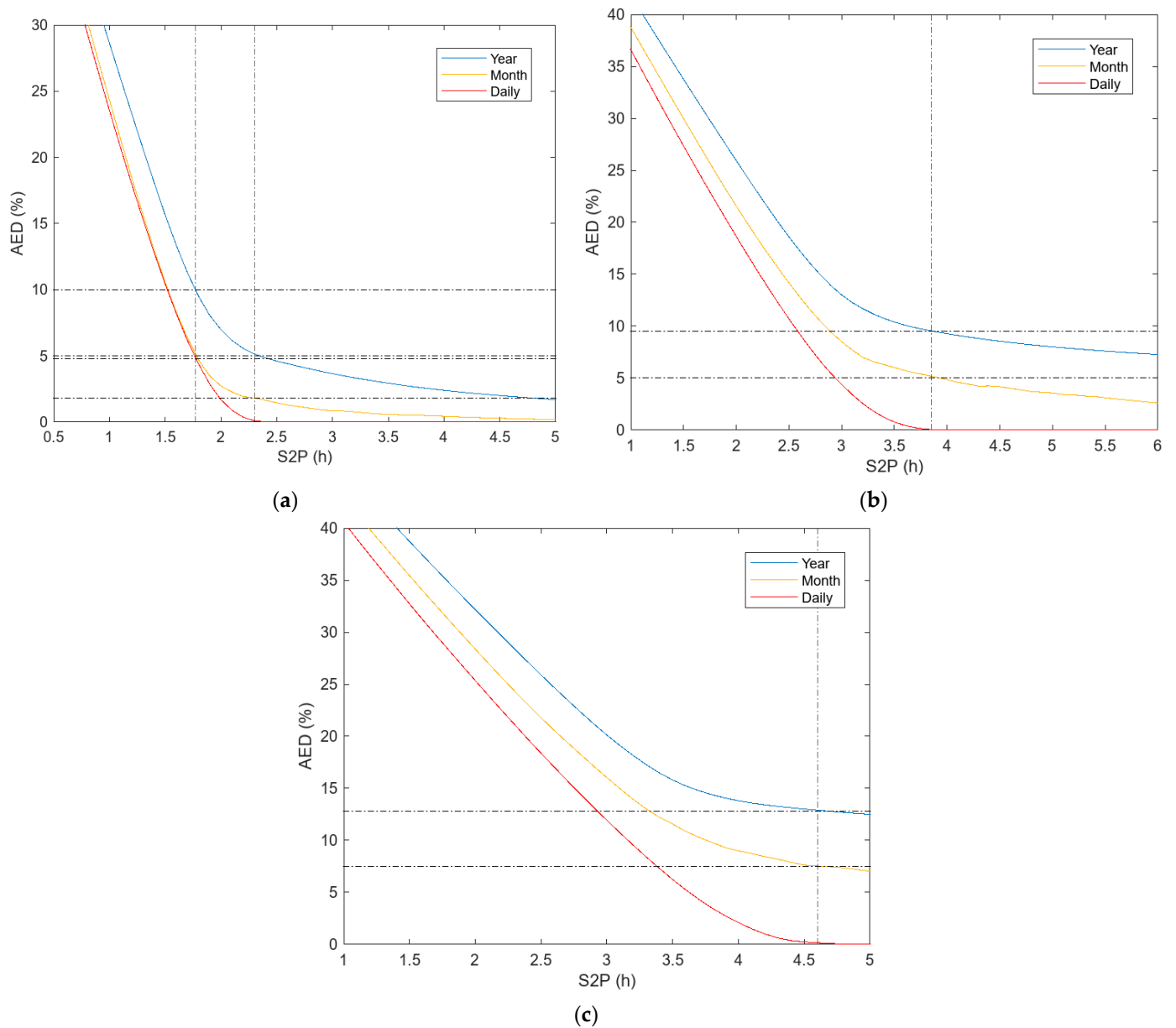


Figure 11. AED comparison for annual, monthly and daily constant power. (a) $K_{SUPPLY} = 0.56$; (b) $K_{SUPPLY} = 0.9$; (c) $K_{SUPPLY} = 1$.

In the present study, a direct relationship is established between the K_{SUPPLY} variable and the CPO_F variable, which was used in previous studies in the same line of research [23,24].

In particular, it has been quantified that a PV plant located in the proposed location produces an annual energy equivalent to a capacity factor or CPO_F of 0.178. Therefore, a CPO_F coefficient of 0.178 is equivalent to selecting a K_{SUPPLY} setpoint of 1, which means that all the energy generated by the PV plant is delivered to the electricity system in the form of constant power. Proportionally, selecting a CPO_F of 0.1 is equivalent to a K_{SUPPLY} setpoint of 0.56 and selecting a CPO_F of 0.16 is equivalent to a K_{SUPPLY} setpoint of 0.9.

Figure 11a shows the AED indicator for an intermediate power setpoint ($K_{SUPPLY} = 0.56$). When analysing the evolution of the daily setpoint, there is a flat area, which means that an increase in storage does not improve the AED indicator. This situation reflects that the system reaches an asymptotic trend, where there are no benefits from increasing storage. It can be concluded that it is not necessary to select an S2P value higher than 2.3 to reduce

energy deficits and meet the scheduled constant power supply requirement. However, these results are unfeasible when considering an annual setpoint. In this case, even with oversized $S2P$ values, it is not possible to completely eliminate energy unavailabilities. Similarly, for monthly setpoints, the results show that a significant oversizing of the storage system, with $S2P$ values in the vicinity of 6, would be required to cancel the energy unavailability.

Furthermore, in the results presented in Figure 11a, it is observed that the use of $S2P$ values lower than 2 does not provide significant improvements when comparing a daily setpoint with a monthly or annual setpoint. Specifically, for an $S2P$ value of 1.7, the AED indicator in the annual setpoint is around 10%, while for the monthly and daily setpoints, this percentage is slightly reduced to approximately 5%. These results make it possible to identify an optimum storage size around $S2P$ of 2.3. From this value onwards, energy unavailability is reduced to zero, making it unnecessary to oversize the storage system. On the other hand, values lower than 1.7 are not recommended, as the AED indicator does not show a significant improvement compared to the monthly and annual setpoints.

Figure 11b plots the AED indicator for a high power setpoint ($K_{SUPPLY} = 0.9$). Similar to the results in Figure 11a, an optimal storage size ($S2P = 3.8$) is identified, from which energy unavailability is completely eliminated under a daily setpoint. However, these levels of AED are unfeasible to achieve with an annual or monthly setpoint. Although the storage value required is relatively high, it is important to note that this configuration allows 90% of the plant's PV production to be supplied daily in the form of constant power, with a total guarantee of supply, as there are no unavailabilities. For the $S2P$ value, which cancels out energy unavailability in the daily setpoint, the AED indicator is 5% in the monthly setpoint and reaches almost 10% in the annual setpoint.

Figure 11c shows the AED indicator for the maximum power setpoint ($K_{SUPPLY} = 1$). This means that all PV production generated during the day is delivered as constant power. The results obtained are consistent and proportionate with Figure 11b, where it is evident that an $S2P$ storage size of 4.6 can completely nullify energy unavailability. This storage size, although oversized, guarantees that all the production generated in the PV plant can be supplied as constant power throughout the day. However, these results would be unfeasible for a monthly and annual setpoint.

The curves presented in Figure 12 are intended to provide an overview of the excess energy generated by the PV plant that cannot be fed into the grid in the form of constant power (but the energy could be injected into the grid, obtaining an economic input). To evaluate these excesses, the AEE indicator is used, which computes the excess energy accumulated until the storage system reaches its end of life. This indicator makes it possible to quantify the energy not used during the operation of the system. The three graphs in Figure 12 show that for any size of storage, the AEE indicator is lower under a daily setpoint compared to a monthly or annual setpoint.

Figure 12a shows the AEE indicator for an intermediate power setpoint ($K_{SUPPLY} = 0.56$). When analysing the evolution of the daily setpoint, it can be concluded that it is not necessary to select a value of $S2P$ higher than 2.3 to reduce excess energy. In Figure 12a, with an intermediate power setpoint for the daily scenario, a sum of energy to be supplied up to EoL of 7.03 GWh is obtained. The output of the PV plant up to EoL (E_{PV}) is 13.23 GWh. Even in the most favourable scenario, with sufficient storage capacity, 6.20 GWh are lost in surplus. This result arises from the difference between the 13.23 GWh of PV production and the 7.03 GWh of power consignment. Therefore, the AEE indicator shows that it is impossible to reduce AEE below 88%. This AEE value coincides with the flat zone previously described. It should be noted that, in the daily setpoint shown in Figure 11a, the saturation elbow from which it is not convenient to increase the $S2P$ value in order to improve the energy indicators is situated in similar values for both the AED and AEE indicators. For monthly and annual setpoints, AEE is slightly higher for $S2P$ of 2.3, as shown in Figure 12a.

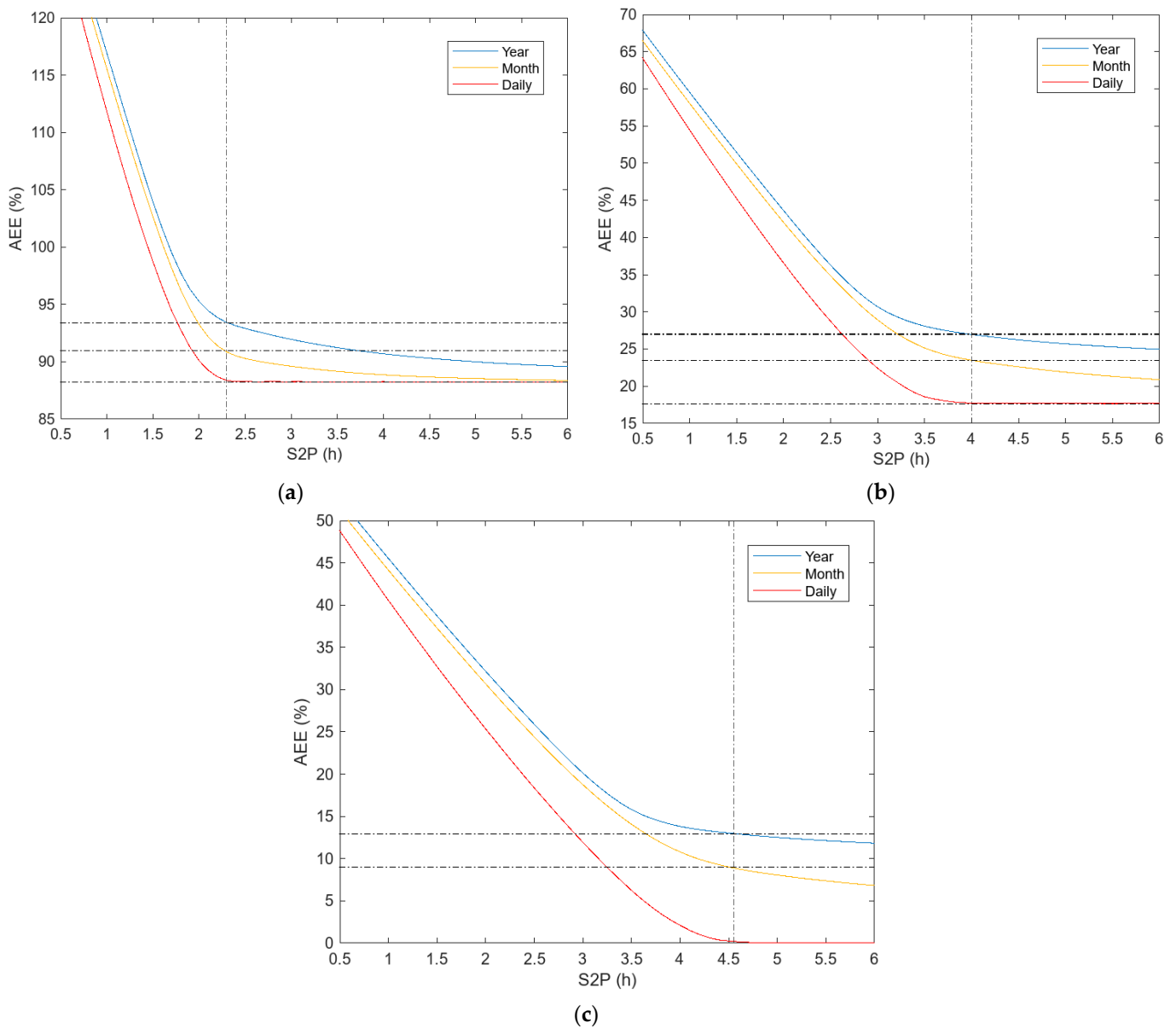


Figure 12. Comparison of AEE for annual, monthly and daily constant power. (a) $K_{SUPPLY} = 0.56$; (b) $K_{SUPPLY} = 0.9$; (c) $K_{SUPPLY} = 1$.

Figure 12b shows the AEE indicator for a high power setpoint ($K_{SUPPLY} = 0.9$). Similar to the case in Figure 12a, a flat zone with an AEE of 17% is distinguished for the daily setpoint when the S2P parameter reaches a value of 4. By applying the same reasoning as in the intermediate setpoint case, it is concluded that AEE should be at least 17% because the power setpoint is lower than the generation capacity of the PV plant. Both AED and AEE reach the saturation bend around an S2P value of 4, which highlights that reducing unavailability reduces the excess energy in the same proportion. It can be assumed that an S2P value of 4 would be adequate for this power setpoint.

The most demanding scenario is shown in Figure 12c, where K_{SUPPLY} reaches its maximum value of 1. In this case, an S2P size larger than 4.6 completely eliminates energy surpluses.

Although this size is relatively high, it is important to note that it allows for achieving the ambitious goal of supplying constant power using the entire PV production of the day. Therefore, selecting an S2P value equal to 4.6 would be the optimal point to guarantee that there are neither energy surpluses nor energy deficits, ensuring that all the energy

produced is converted into constant, firm power. Under the same conditions, but in the monthly and annual setpoint, this situation is unfeasible because the AEE in the monthly setpoint is 9% and in the annual setpoint 13%.

To summarise the main idea presented in this section and facilitate the selection of the optimal storage size, Table 1 presents the selected $S2P$ parameter based on the AED and AEE indicators according to the power setpoint (K_{SUPPLY}). When K_{SUPPLY} is 0.56 (intermediate setpoint), an $S2P$ of 2.3 is optimal for both the AED and AEE indicators. If K_{SUPPLY} is 0.9 (high setpoint), an $S2P$ of 3.8 is recommended according to the AED indicator and an $S2P$ of 4 according to the AEE indicator. For K_{SUPPLY} equal to 1 (setpoint equivalent to photovoltaic production), an $S2P$ of 4.6 is the appropriate size according to both indicators.

Table 1. Optimal selection of the $S2P$ parameter based on the power setpoint of AED and the AEE indicator.

K_{SUPPLY}	AED	AEE
0.56	2.3	2.3
0.9	3.8	4
1	4.6	4.6

In the scenario where all PV production is intended to be supplied as constant power ($K_{SUPPLY} = 1$), it is observed that the indicators AED in Figure 11c and AEE in Figure 12c present practically equivalent values. In order to better understand this coincidence, a more detailed analysis of the results is carried out below. The similarity between the two indicators could suggest a direct compensation between the energy not supplied as constant power and the excess energy that cannot be absorbed by the storage system. This would indicate an almost perfect balance between the energy that is missing to meet the constant power setpoint and the energy that is lost due to storage capacity limitations.

If the size of the storage system is not sufficient to transform all daily generation into constant power, the SoC of the BESS fluctuates between its maximum and minimum values. This dynamic causes power unavailability before sunrise, which is roughly equivalent to the excess power produced during sunset. As an example of this behaviour, Figure 13 illustrates the evolution of the system during a typical 96-h period with high PV production. In this figure, the blue curve (BESS) represents the stored energy, the red curve (PV) represents the PV energy production, the yellow bars (DEF) quantify the hourly unavailable energy and the purple bars (SUR) show the hourly energy surpluses. As can be seen, there is a clear similarity between the daily deficits and surpluses, indicating a symmetry between the unutilised energy and the missing energy, caused by the storage size limitation.

This situation remains constant throughout the simulation. Figure 14 presents a longer period of 20 days during the month of June, a month characterised by high PV production. For each day, the red bars (PV) represent the PV production, the blue bars (DEF) show the energy deficit, and the yellow bars (SUR) reflect the energy surplus. As can be seen, the pattern of energy deficit and surplus is similar each day, indicating that this behaviour is neither an isolated phenomenon nor dependent on specific weather conditions.

To provide an overview of the daily energy supplied, Figure 15 presents the average daily power setpoint to be supplied in the simulation up to the end of life of the BESS, in contrast to the representation of multiple days in Figure 13 or a single month in Figure 14. The series shows high variability between the minimum and maximum setpoints. The system reaches almost 250 kW of constant power supply in summer, while in December, the guaranteed power drops to approximately 100 kW. This minimum value can be considered as the minimum guaranteed power from the plant or the firm power that this system can reliably supply.

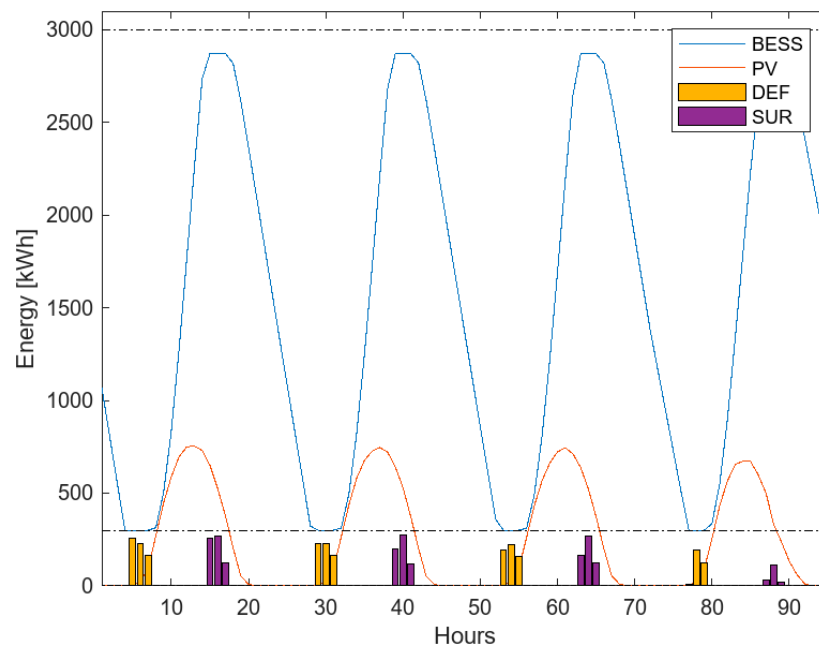


Figure 13. Hourly energy balance in BESS, PV generation and energy deviations.

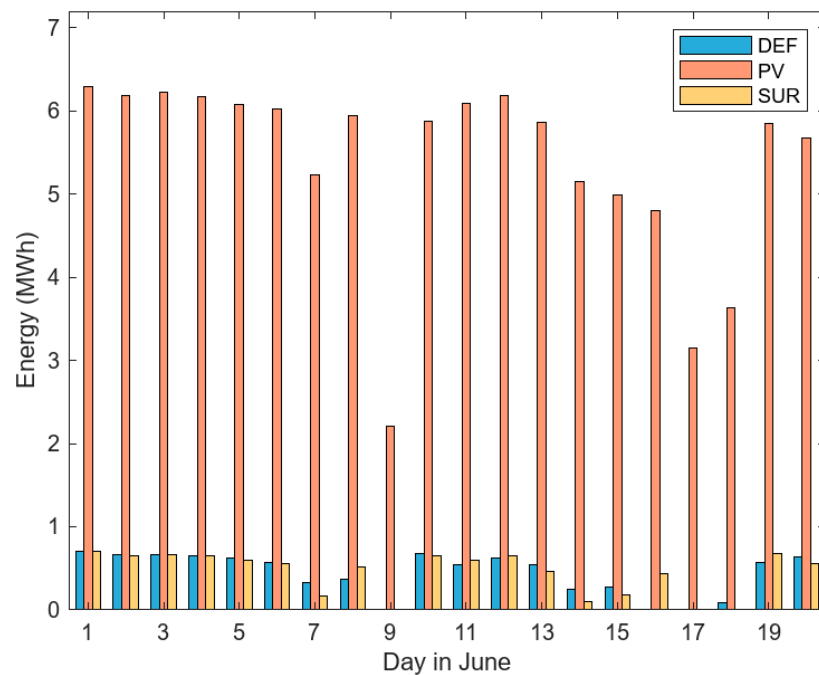


Figure 14. Daily energy generated, system deficits and surpluses.

Figure 16 presents the generation duration curve of the energy intended to be supplied. This monotonically decreasing curve is a graphical representation where the value of the dependent variable decreases or remains constant as the independent variable increases, with no increases at any point. In this case, the graph reorganises the same results from Figure 15 but is ordered by the percentage occurrence of each power level over time. For example, a firm power of 205 kW is guaranteed 50% of the time, while a minimum value of 100 kW is guaranteed 100% of the time. This latter value, as mentioned in Figure 15, represents the firm power that the system can consistently supply.

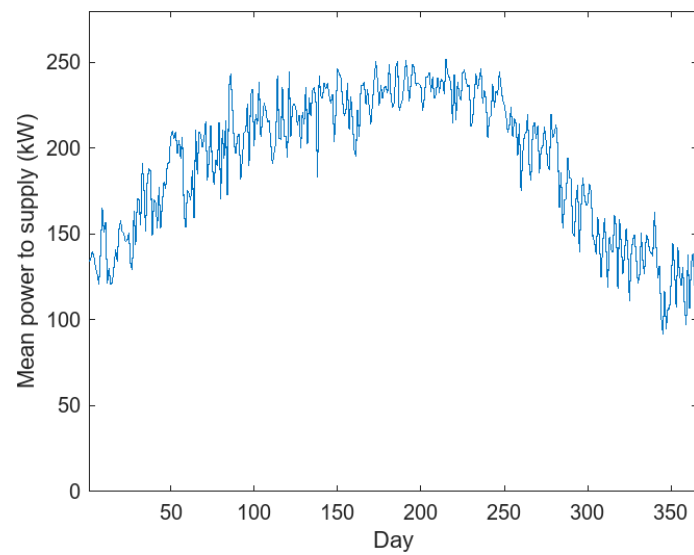


Figure 15. Average power setpoint to be supplied by day of the year up to the end of life of the BESS.

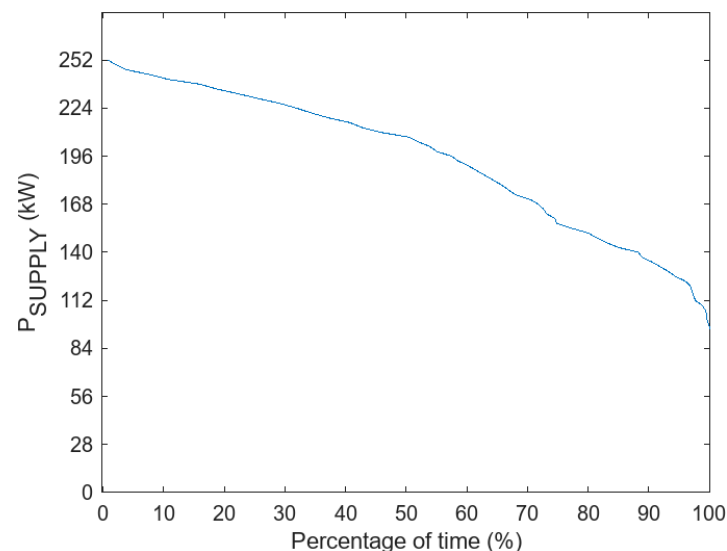


Figure 16. Generation duration curve of energy to be supplied for each day of the year.

4. Conclusions

This study has made it possible to evaluate the energy performance of a PV plant with battery storage to supply constant power 24 h a day. By properly sizing the storage system and using accurate daily forecasts of PV production, it has been demonstrated that it is possible to transform variable solar power generation into a constant and reliable supply.

The results obtained conclude that an $S2P$ (storage size) of 4.6 is able to completely eliminate energy unavailability ($AED = 0$) by supplying all PV production as constant power ($K_{SUPPLY} = 1$).

For each power setpoint, an optimal $S2P$ value has been found at which energy unavailability is completely eliminated or no longer decreases significantly. It has also been shown that the strategy of adjusting the power setpoint on a daily basis, rather than monthly or yearly, significantly improves energy availability. In addition, oversizing storage appropriately has been shown to have other benefits, such as reducing storage degradation and reducing energy surpluses.

Although the energy results are positive, large-scale implementation of PV-BESS systems for a constant supply remains a challenge, mainly due to the current high cost of

batteries. However, continuing cost decreases and technological advances in the field of energy storage indicate that this solution could become economically viable in the near future. This could redefine the role of solar PV, converting it from an intermittent to a dispatchable and reliable source and contributing significantly to the transition towards more sustainable and resilient energy systems.

Author Contributions: Conceptualisation, J.A.T.-G. and Á.A.B.-R.; methodology, J.A.T.-G.; software, J.A.T.-G.; validation, J.A.T.-G. and Á.A.B.-R.; formal analysis, J.A.T.-G.; investigation, J.A.T.-G. and Á.A.B.-R.; resources, J.A.T.-G.; data curation, J.A.T.-G.; writing—original draft preparation, Á.A.B.-R.; writing—review and editing, Á.A.B.-R.; visualisation, J.A.T.-G.; supervision, Á.A.B.-R. All authors have read and agreed to the published version of the manuscript.

Funding: This research received no external funding.

Data Availability Statement: Data are contained within the article.

Conflicts of Interest: The authors declare no conflicts of interest. The funders had no role in the design of the study; in the collection, analyses, or interpretation of data; in the writing of the manuscript; or in the decision to publish the results.

Abbreviations

AED	annual energy deviation
AEE	annual energy excess
BESS	battery energy storage system
C_{LOSS}	loss coefficient
CO_2	carbon dioxide
C_{MAX}	BESS capacity
CPO_F	constant power operation factor
$E_{B,t}$	energy in battery
E_{GRID}	energy supplied
E_{PV}	photovoltaic production
G_M	average irradiance
G_{STC}	irradiance under STC conditions
IEA	International Energy Agency
IRENA	International Renewable Energy Agency
LCOE	levelised cost of energy
MED	monthly energy deviation
NOCT	nominal operating cell temperature
N_P	number of modules
$P_{BC,t}$	battery power
P_{MOD}	module power
P_N	nominal power
P_P	peak power of photovoltaic plant
PV	photovoltaic
PVGIS	photovoltaic geographical information system
SoC	state of charge
SoH	state of health
T_A	ambient temperature
T_C	cell temperature
T_S	sampling time
Δt	time step
γ	temperature coefficient
$\eta_{B,EF}$	round-trip efficiency
$\eta_{B,inv}$	inverter efficiency
σ	self-discharge

References

1. Renewables Global Status Report 2021. REN21 Renewables Now. Available online: <https://ren21.net/gsr-2021/> (accessed on 26 September 2024).
2. Net Zero by 2050. A Roadmap for the Global Energy Sector International Energy Agency. Available online: <https://www.iaea.org/reports/net-zero-by-2050> (accessed on 22 September 2024).
3. International Renewable Energy Agency (IRENA). World Energy Transitions Outlook 2022. Available online: <https://www.irena.org/Digital-Report/World-Energy-Transitions-Outlook-2022> (accessed on 22 September 2024).
4. The Paris Agreement on Climate Change 2015. Available online: https://unfccc.int/sites/default/files/spanish_paris_agreement.pdf (accessed on 24 September 2024).
5. United Nations Resolution 70/1. Transforming Our World: The 2030 Agenda for Sustainable Development, Adopted by the General Assembly on 25 September 2015. Available online: <https://undocs.org/en/A/RES/70/1> (accessed on 25 September 2024).
6. International Renewable Energy Agency (IRENA). Renewable Statistics 2024. Available online: https://www.irena.org/-/media/Files/IRENA/Agency/Publication/2024/Jul/IRENA_Renewable_Energy_Statistics_2024.pdf (accessed on 24 September 2024).
7. International Renewable Energy Agency (IRENA). Renewable Power Generation Costs in 2023. Available online: https://www.irena.org/-/media/Files/IRENA/Agency/Publication/2024/Sep/IRENA_Renewable_power_generation_costs_in_2023.pdf (accessed on 24 September 2024).
8. O'Shaughnessy, E.; Cruce, J.R.; Xu, K. Too much of a good thing? Global trends in the curtailment of solar PV. *Sol. Energy* **2020**, *208*, 1068–1077. [[CrossRef](#)] [[PubMed](#)]
9. Beltran, H.; Cardo-Miota, J.; Segarra-Tamarit, J.; Pérez, E. Battery size determination for photovoltaic capacity firming using deep learning irradiance forecasts. *J. Energy Storage* **2021**, *33*, 102036. [[CrossRef](#)]
10. Brahmendra Kumar, G.V.; Palanisamy, K.; Sanjeevikuman, P.; Muyeen, S.M. Analysis of control strategies for smoothing of solar PV fluctuations with storage devices. *Energy Rep.* **2023**, *9*, 163–177. [[CrossRef](#)]
11. Lund, P.D.; Lindgren, J.; Mikkola, J.; Salpakari, J. Review of energy system flexibility measures to enable high levels of variable renewable electricity. *Renew. Sustain. Energy Rev.* **2015**, *45*, 785–807. [[CrossRef](#)]
12. Office of Energy Efficiency & Renewable Energy. U.S. Department of Energy. Solar Futures Study. 2021. Available online: <https://www.energy.gov/eere/solar/solar-futures-study> (accessed on 25 September 2024).
13. Kebede, A.A.; Kalogiannis, T.; Van Mierlo, J.; Bercibar, M. A comprehensive review of stationary energy storage devices for large scale renewable energy sources grid integration. *Renew. Sustain. Energy Rev.* **2020**, *159*, 112213. [[CrossRef](#)]
14. Armand, M.; Axmann, P.; Bresser, D.; Copley, M.; Edström, K.; Ekberg, C.; Guyomard, D.; Lestriez, B.; Novák, P.; Petranikova, M.; et al. Lithium-ion batteries—Current state of the art and anticipated developments. *J. Power Sources* **2020**, *479*, 228708. [[CrossRef](#)]
15. Gupta, R.; Soini, M.C.; Patel, M.K.; Parra, D. Levelized cost of solar photovoltaics and wind supported by storage technologies to supply firm electricity. *J. Energy Storage* **2020**, *27*, 101027. [[CrossRef](#)]
16. Maleki, M.; El-Nagar, G.; Bernsmeier, D.; Schneider, J.; Roth, C. Fabrication of an efficient vanadium redox flow battery electrode using a free-standing carbon-loaded electrospun nanofibrous composite. *Nature* **2020**, *10*, 11153. [[CrossRef](#)]
17. Freire-Barceló, T.; Martín-Martínez, F.; Sánchez-Mirallas, A.; Rivier, M.; Gómez, T.; Huclin, S.; Chaves, J.P.; Ramos, A. Storage and demand response contribution to firm capacity: Analysis of the Spanish electricity system. *Energy Rep.* **2022**, *8*, 10546–10560. [[CrossRef](#)]
18. Perez, M.; Perez, R.; Rábago, K.R.; Putnam, M. Overbuilding & curtailment: The cost-effective enablers of firm PV generation. *Sol. Energy* **2019**, *180*, 412–422. [[CrossRef](#)]
19. Ramadhan, M.F.; Azmi, R.M.; Supriyadi, E.; Agustian, W.; Sastrowijoyo, F. PV Intermittent Smoothing with BESS: A Case Study in Selayar Island Electrical Grid. In Proceedings of the 5th International Conference on Power Engineering and Renewable Energy, Bandung, Indonesia, 22–23 November 2022. [[CrossRef](#)]
20. Fattori, F.; Anglani, N.; Staffell, I.; Pfenninger, S. High solar photovoltaic penetration in the absence of substantial wind capacity: Storage requirements and effects on capacity adequacy. *Energy* **2017**, *137*, 193–208. [[CrossRef](#)]
21. BloombergNEF, 2H 2023 Levelized Cost of Electricity Update. 2023. Available online: <https://about.bnef.com/blog/2h-2023-lcoe-update-an-uneven-recovery> (accessed on 7 October 2024).
22. Bayod-Rújula, A.A.; Tejero-Gómez, J.A. Analysis of the hybridization of PV plants with BESS for Annual Constant Power Operation. *Energies* **2022**, *15*, 9063. [[CrossRef](#)]
23. Tejero-Gómez, J.A.; Bayod-Rújula, A.A. Analysis of Photovoltaic Plants with Battery Energy Storage Systems (PV-BESS) for Monthly Constant Power Operation. *Energies* **2023**, *16*, 4909. [[CrossRef](#)]
24. Tejero-Gómez, J.A.; Bayod-Rújula, A.A. Sizing of Battery Energy Storage Systems for firming PV power including aging analysis. *Energies* **2024**, *17*, 1485. [[CrossRef](#)]
25. Mercado de Electricidad OMIE. Available online: <https://www.omie.es/es/mercado-de-electricidad> (accessed on 1 October 2024).
26. The MathWorks, Inc. *MATLAB*; Versión R2023a; The MathWorks, Inc.: Natick, MA, USA, 2023.
27. Photovoltaic Geographical Information Systema. Available online: https://re.jrc.ec.europa.eu/pvg_tools/en (accessed on 8 October 2024).

28. Solar Module Series 7 TR1 525-550W Thin Film Solar Module. First Solar. Available online: <https://www.firstsolar.com/-/media/First-Solar/Technical-Documents/Series-7/Series-7-TR1-High-Bin-Datasheet.ashx?la=en> (accessed on 9 October 2024).
29. Mangherini, G.; Diolaiti, V.; Bernardoni, P.; Andreoli, A.; Vincenzi, D. Review of Façade Photovoltaic Solutions for Less Energy-Hungry Buildings. *Energies* **2023**, *16*, 6901. [[CrossRef](#)]
30. Alrumayh, O.; Sayed, K.; Almutairi, A. LVRT and Reactive Power/Voltage Support of Utility-Scale PV Power Plants during Disturbance Conditions. *Energies* **2023**, *16*, 3245. [[CrossRef](#)]
31. Fantham, T.L.; Gladwin, D.T. Impact of cell balance on grid scale battery energy storage systems. *Energy Rep.* **2020**, *6*, 209–216. [[CrossRef](#)]
32. Peng, S.; Zhu, J.; Wu, T.; Tang, A.; Kan, J.; Pecht, M. SOH early prediction of lithium-ion batteries based on voltage interval selection and features fusion. *Energy* **2024**, *308*, 132993. [[CrossRef](#)]
33. Ahmed, R.; Sreeram, V.; Mishra, Y.; Arif, M.D. A review and evaluation of the state-of-the-art in PV solar power forecasting: Techniques and optimization. *Renew. Sustain. Energy Rev.* **2020**, *124*, 109792. [[CrossRef](#)]
34. Voyant, C.; Notton, G.; Kalogirou, S.; Nivet, M.; Paoli, C.; Motte, F.; Fouilloy, A. Machine learning methods for solar radiation forecasting: A review. *Renew. Energy* **2017**, *105*, 569–582. [[CrossRef](#)]
35. Li, Y.; Zhou, W.; Wang, Y.; Miao, S.; Yao, W.; Gao, W. Interpretable deep learning framework for hourly solar radiation forecasting based on decomposing multi-scale variations. *Appl. Energy* **2025**, *377*, 124409. [[CrossRef](#)]
36. European Centre for Medium-Range Weather Forecasts (ECMWF). Available online: <https://www.ecmwf.int> (accessed on 8 October 2024).
37. The Mesoscale and Microscale Meteorology. Available online: <https://www.mmm.ucar.edu> (accessed on 8 October 2024).
38. Yang, G.; Yang, D.; Liu, B.; Zhang, H. The role of short- and long-duration energy storage in reducing the cost of firm photovoltaic generation. *Appl. Energy* **2024**, *374*, 123914. [[CrossRef](#)]

Disclaimer/Publisher’s Note: The statements, opinions and data contained in all publications are solely those of the individual author(s) and contributor(s) and not of MDPI and/or the editor(s). MDPI and/or the editor(s) disclaim responsibility for any injury to people or property resulting from any ideas, methods, instructions or products referred to in the content.